Science Advances
AAAS

advances.sciencemag.org/cgi/content/full/5/8/eaax1396/DC1

Supplementary Materials for

Increased atmospheric vapor pressure deficit reduces global vegetation growth

Wenping Yuan*, Yi Zheng, Shilong Piao, Phillipe Ciais, Danica Lombardozzi, Yingping Wang, Youngryel Ryu, Guixing Chen, Wenjie Dong, Zhongming Hu, Atul K. Jain, Chongya Jiang, Etsushi Kato, Shihua Li, Sebastian Lienert, Shuguang Liu, Julia E.M.S. Nabel, Zhangcai Qin, Timothy Quine, Stephen Sitch, William K. Smith, Fan Wang, Chaoyang Wu, Zhiqiang Xiao, Song Yang

*Corresponding author. Email: yuanwp3@mail.sysu.edu.cn

Published 14 August 2019, *Sci. Adv.* **5**, eaax1396 (2019)
DOI: 10.1126/sciadv.aax1396

This PDF file includes:

Table S6. Correlation matrixes for global VPD simulated by the six CMIP5 ESMs and four historical datasets (CRU, ERA-Interim, HadISDH, and MERRA).
Table S7. Model parameters of EC-LUE for different vegetation types.

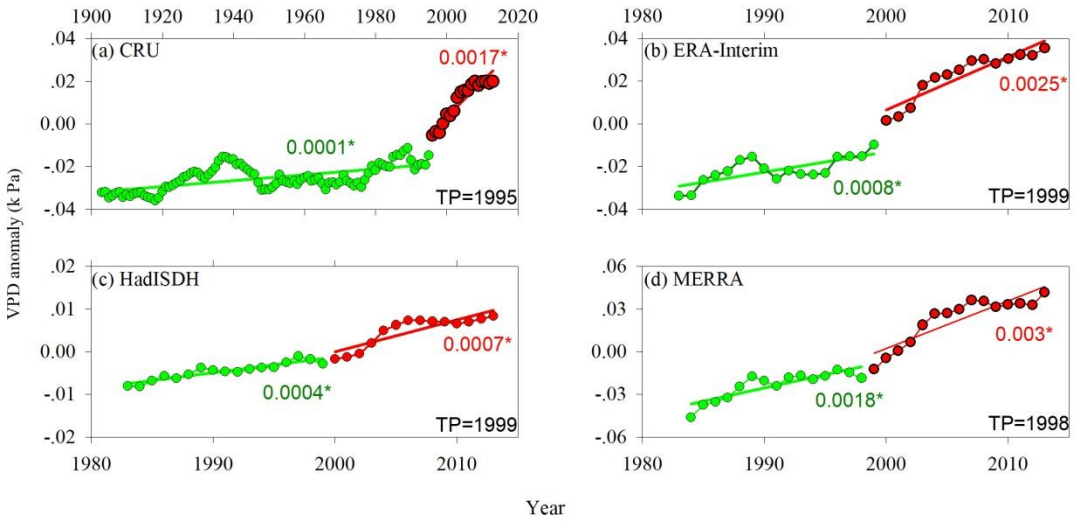

Fig. S1. Five-year moving average of VPD. Green and red lines indicate the linear fit before and after the turning point (TP) years. The numbers show the change rates of VPD (k Pa yr^{-1}), and * indicates the significant changes at a significance level of $p<0.05$.

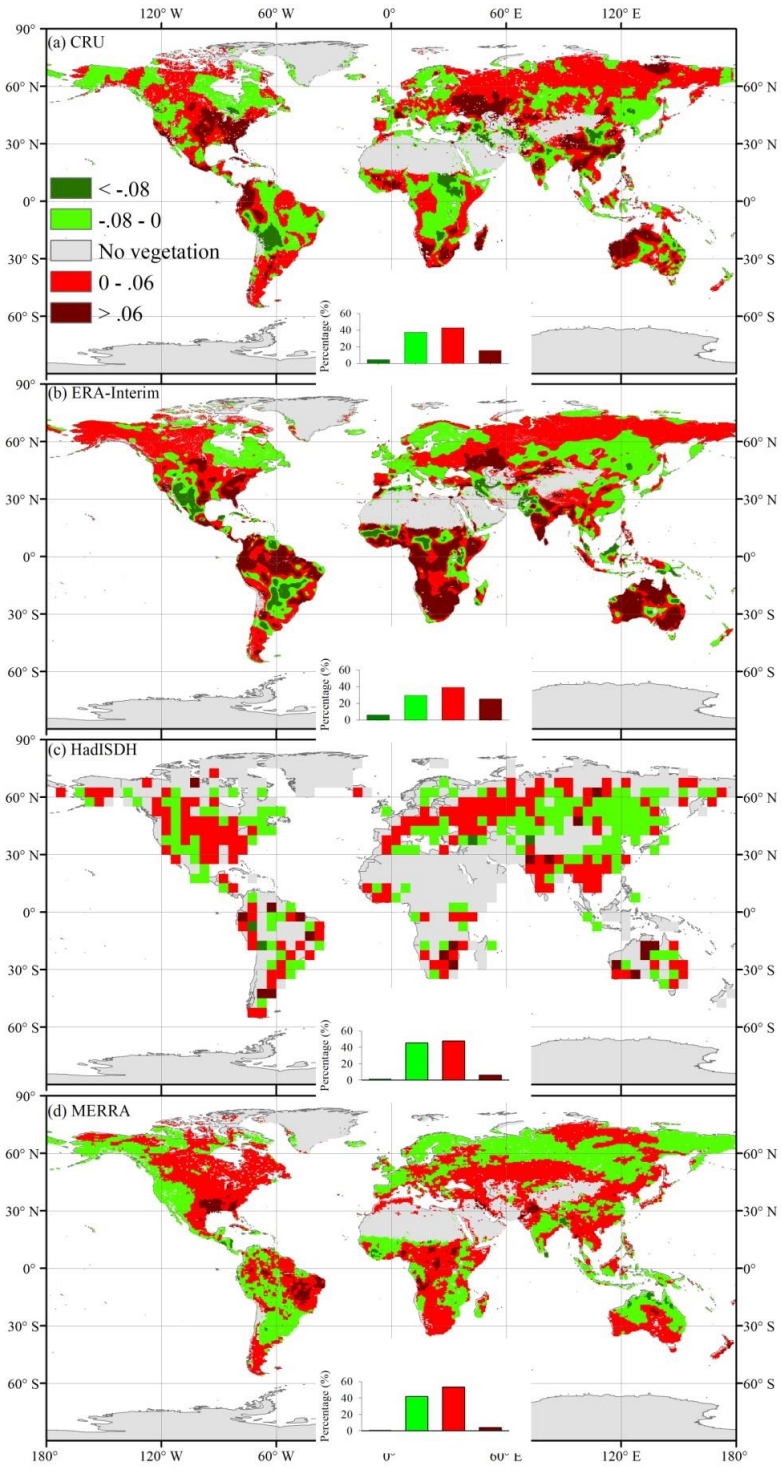

Fig. S2. Spatial distributions of the difference of VPD trends (kPa year^{-1}) before and after TP years. The insets show the frequency distributions of the corresponding differences. Positive values indicate the higher VPD trends after turning point years than before.

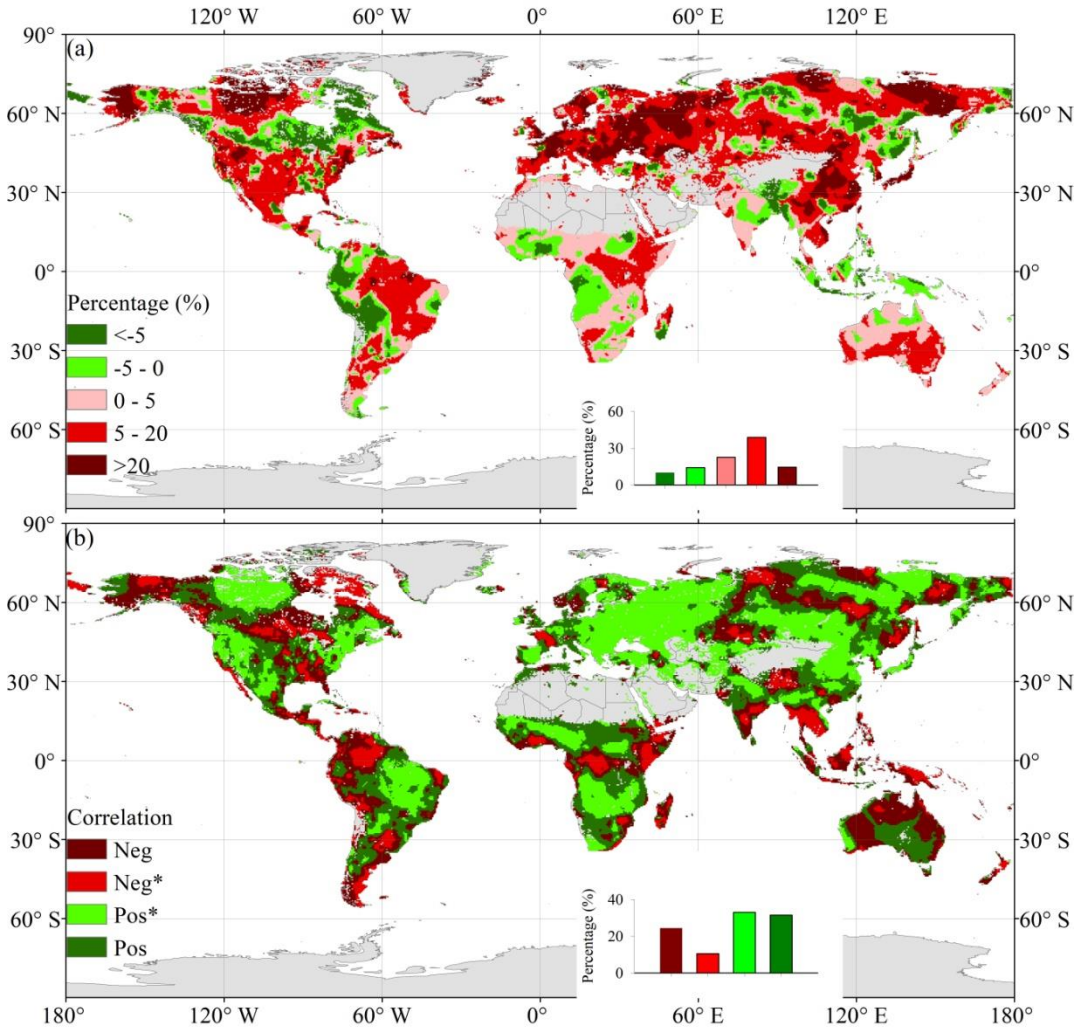

Fig. S3. Spatial pattern of VPD changes between 1982–1986 and 2011–2015 derived from CRU dataset. (**a**) Percentage changes of VPD between 1982-1986 and 2011-2015. The values show the percentage of difference: $(VPD_2\text{-}VPD_1)/VPD_1 \times 100\%$. VPD_1 and VPD_2 are the annual growing season mean VPD values of 1982-1986 and 2011-2015. (**b**) Correlation between monthly mean VPD and VPD differences ($VPD_2\text{-}VPD_1$) over 12 months.

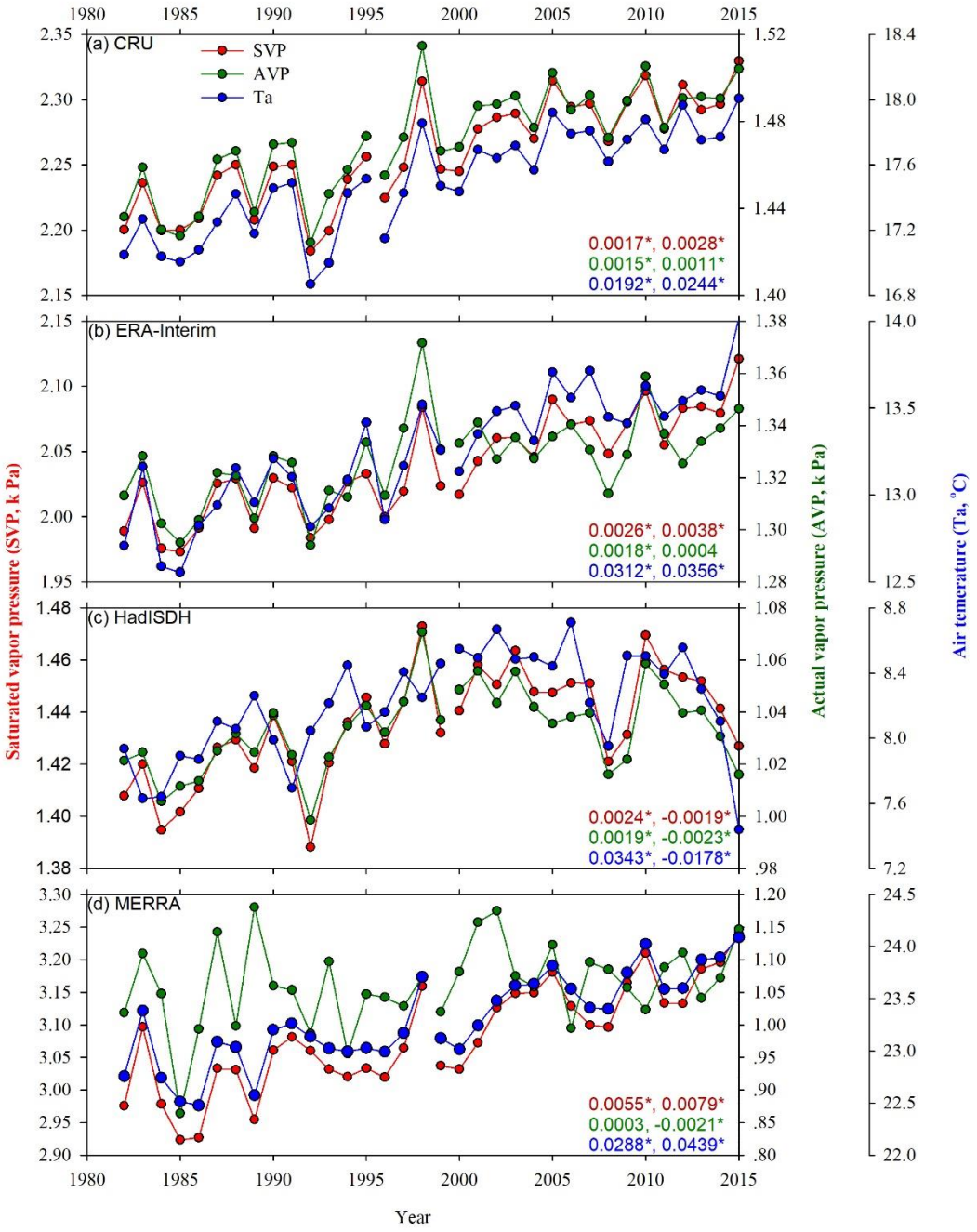

Fig. S4. Interannual variability of SVP (red dots and lines), AVP (green dots and lines), and air temperature (T_a; blue dots and lines) derived from four datasets. The number in the lower right corner of each plot indicate the change trends of SVP (red; k Pa yr^{-1}), AVP (green; k Pa yr^{-1}), and air temperature (blue; ℃ yr^{-1}) before and after the turning point years, respectively, and * shows significant trends at $p<0.05$.

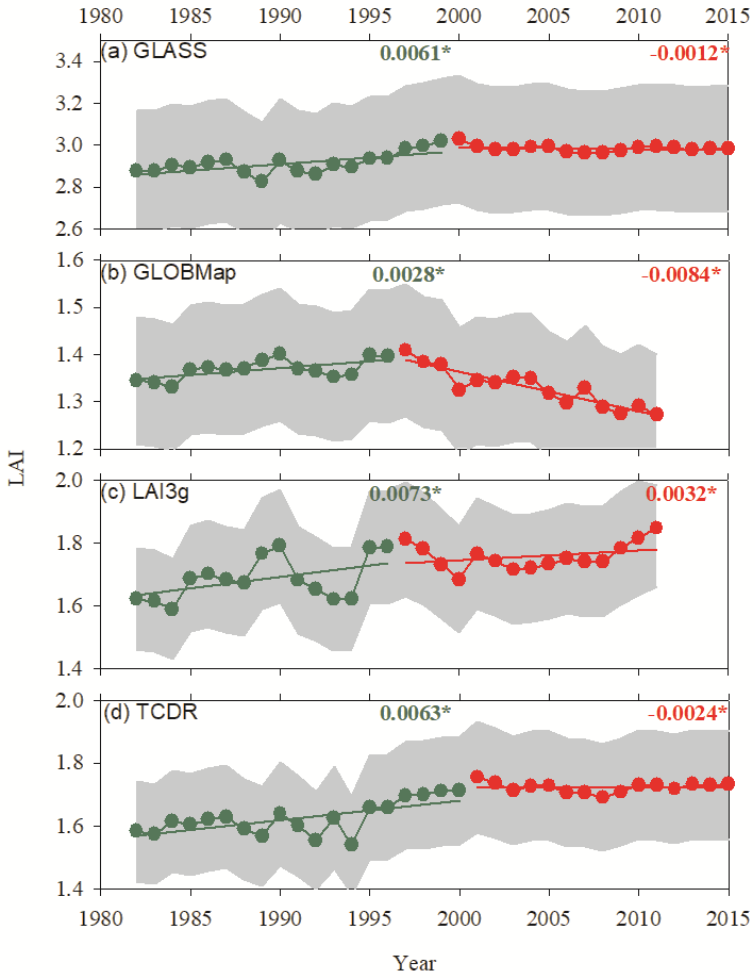

Fig. S5. Global mean LAI and linear trends during 1982–2015. Shaded area indicates the standard deviation. Green and red lines indicate linear fits before and after the turning point years. The numbers show the change rates of LAI, and * indicates the significant changes at a significance level of $p<0.05$.

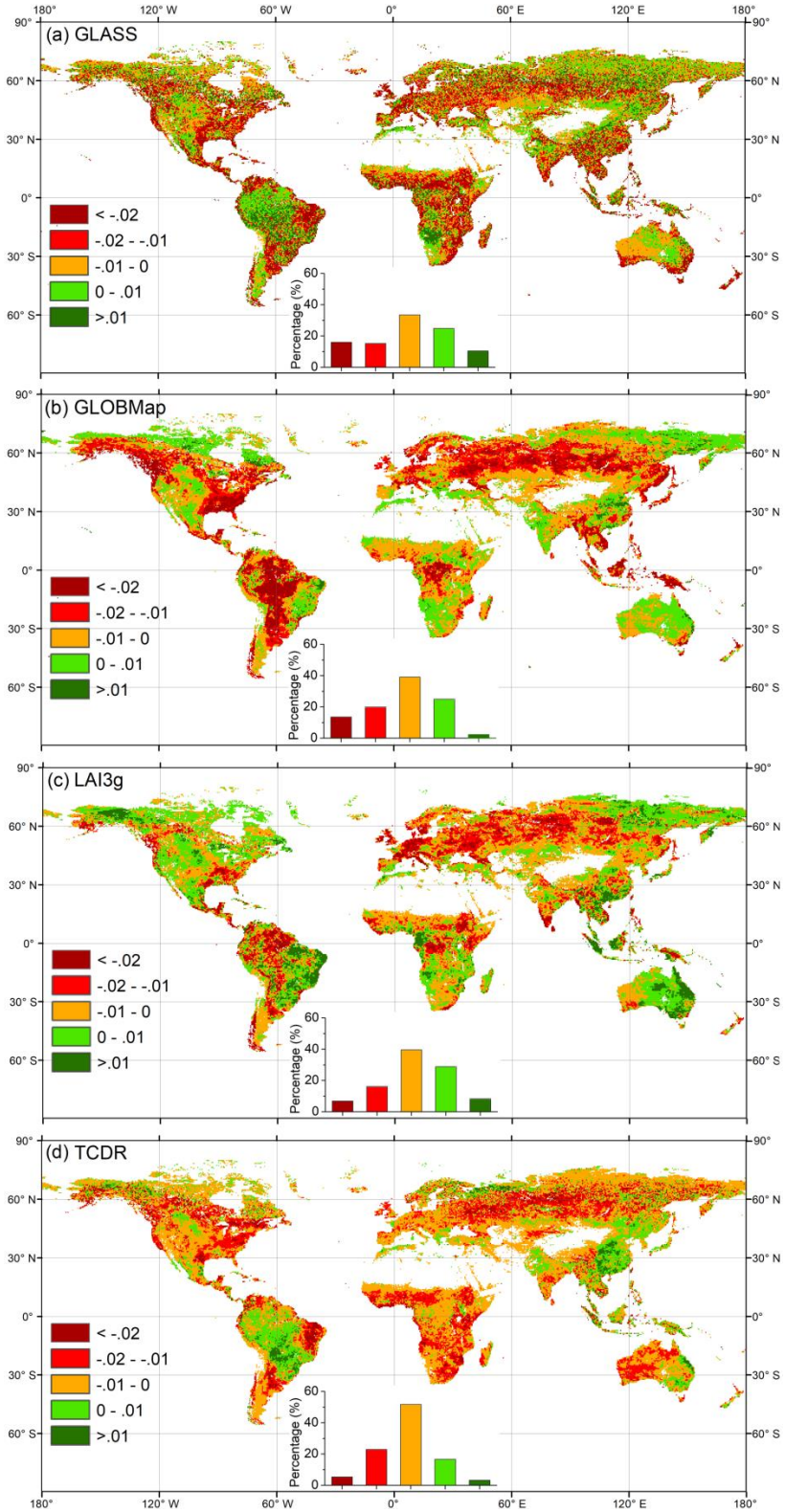

Fig. S6. Differences of LAI trends over the globally vegetated areas between before and after TP years. Insets show the frequency distributions of the corresponding differences. Negative values indicate the lower LAI trends after turning point years than before.

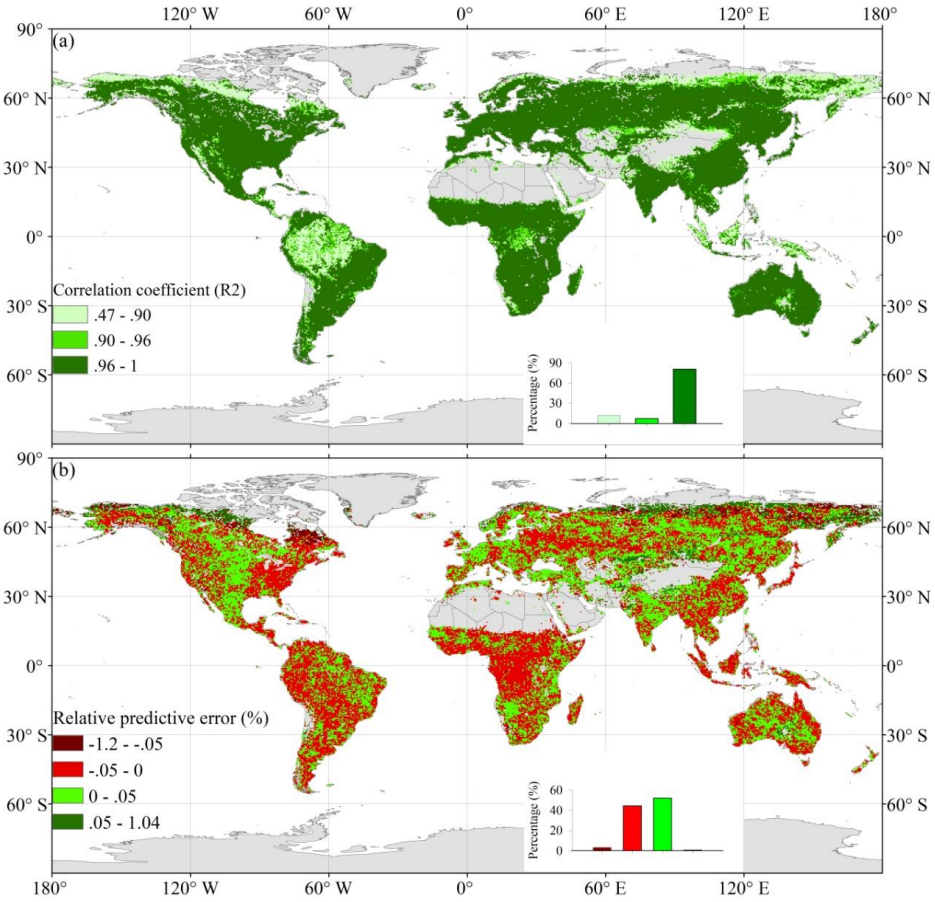

Fig. S7. Model validation of random forest models for simulating NDVI. (**a**) Interannual correlation coefficient (R^2) and (**b**) relative predictive error (RPE, %) (PRE = (S-O)/O, S and O indicate the simulated NDVI and GIMMS3g NDVI values, respectively.)

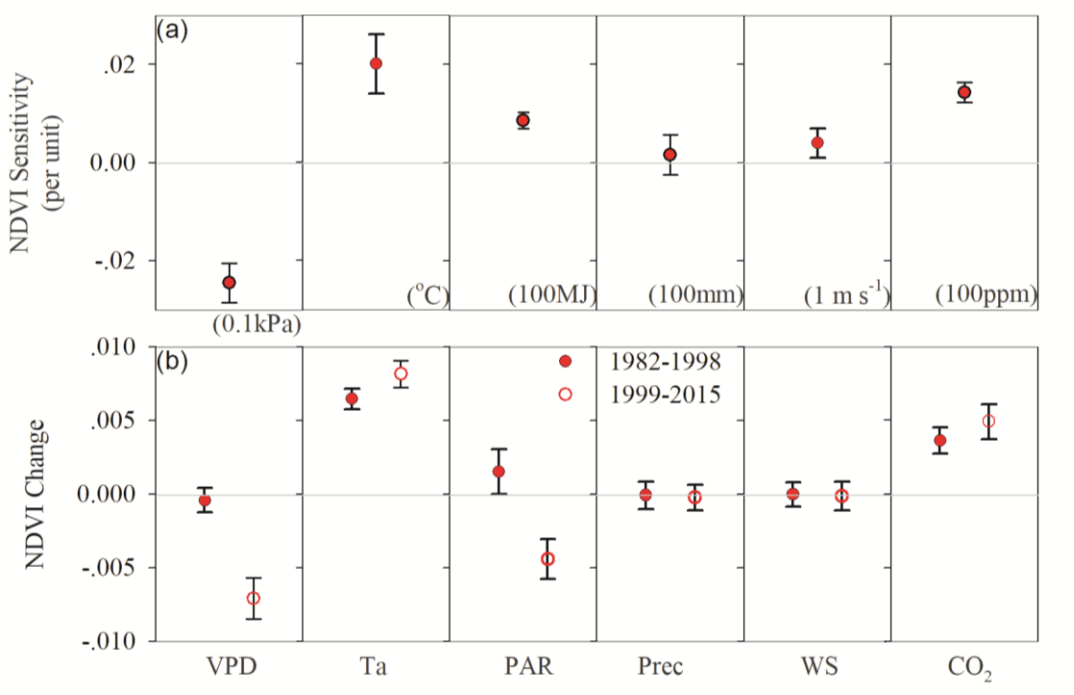

Fig. S8. Environmental regulations on long-term changes of global NDVI. (**a**) NDVI sensitivity to climate variables and atmospheric CO_2 concentration. (**b**) Contributions of climate variables and atmospheric CO_2 concentration (CO_2) to NDVI changes over the two periods. Five climate variables are included: vapor pressure deficit (VPD), air temperature (Ta), photosynthetically active radiation (PAR), precipitation (Prec), and wind speed (WS). The positive values indicate NDVI increases with these variables.

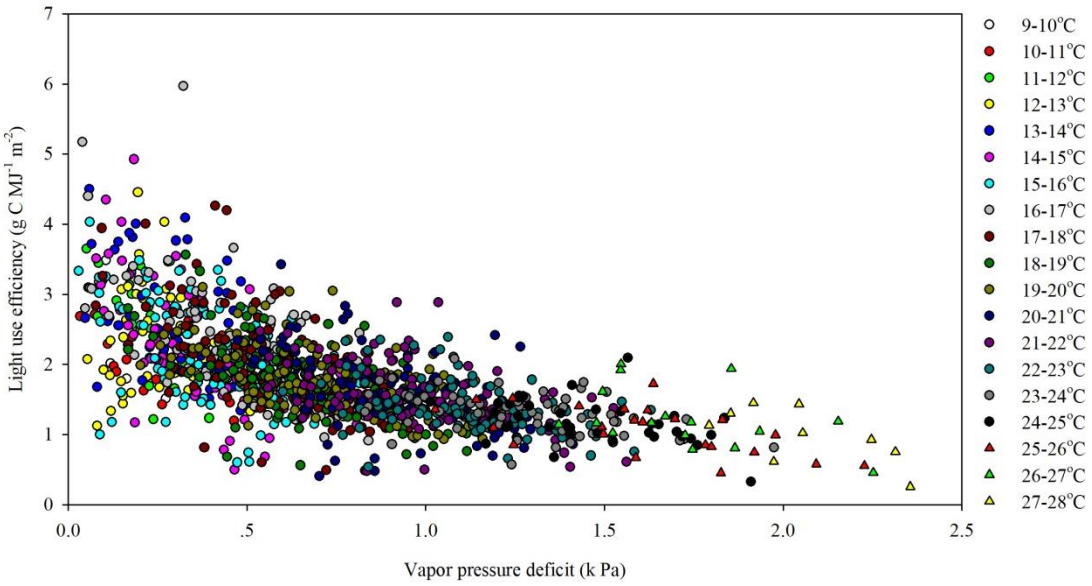

Fig. S9. Correlations of LUE and VPD at the different temperature ranges taking DE-Tha site as an example.

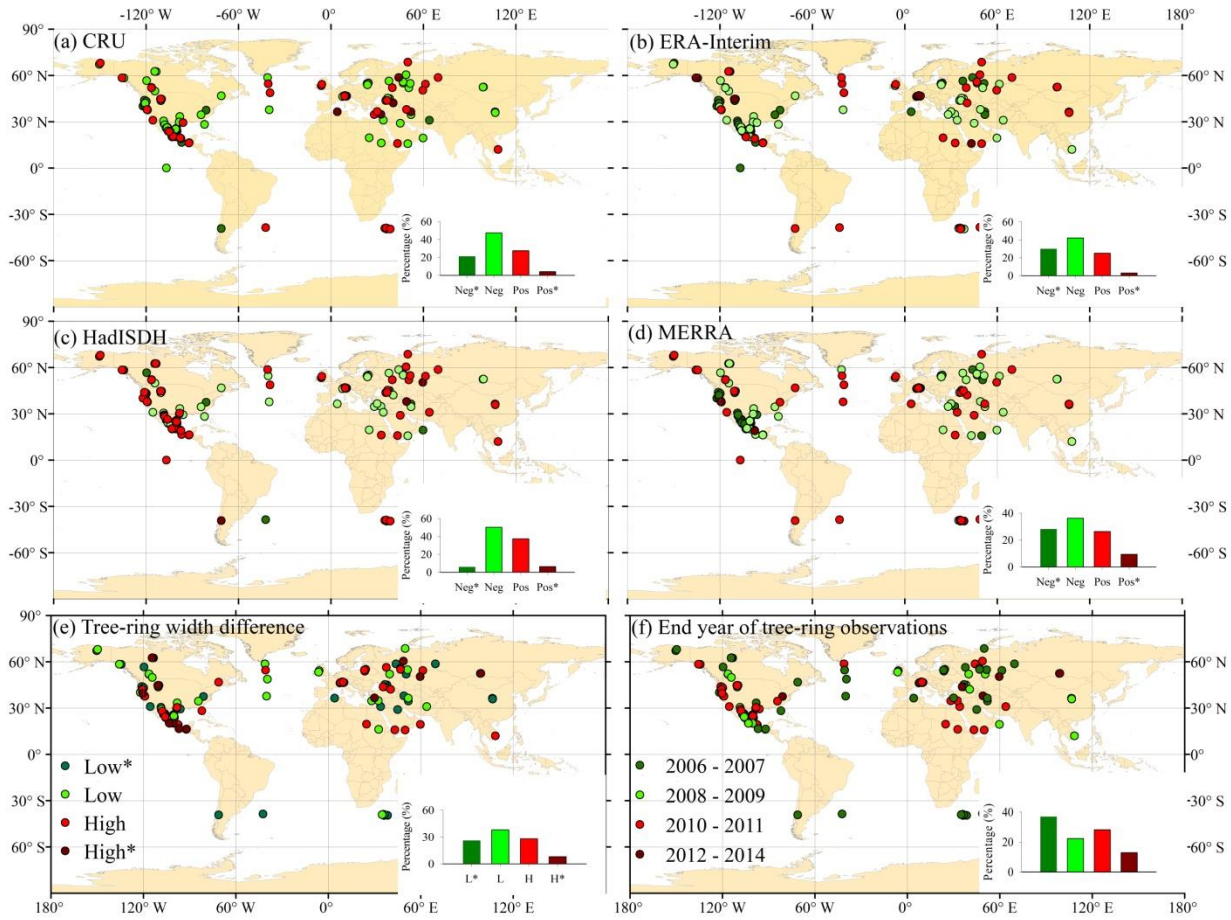

Fig. S10. Correlations between VPD and tree-ring width. (**a**)-(**d**) Partial correlations between detrended tree-ring width and detrended vapor pressure deficit derived from four datasets excluding the impacts of air temperature, radiation and atmospheric CO_2 concentration. Inserts indicate the percentage of four types of correlation (Neg and Pos indicate negative and positive correlations, respectively, and * indicate a significant correlation at the $p<0.05$ level). (**e**) Comparison on mean tree-ring width between two periods (1982-1998 and after 1999). Low and High indicate the lower and higher mean values of tree-ring width after 1999 compared to those of 1982-1998 respectively. * indicates the significant differences between two periods using the t-test ($p<0.05$). Inserts indicate the percentage of four types of differences. (**f**) The end year of tree-ring width observations, and the insert shows the percentage of four time ranges.

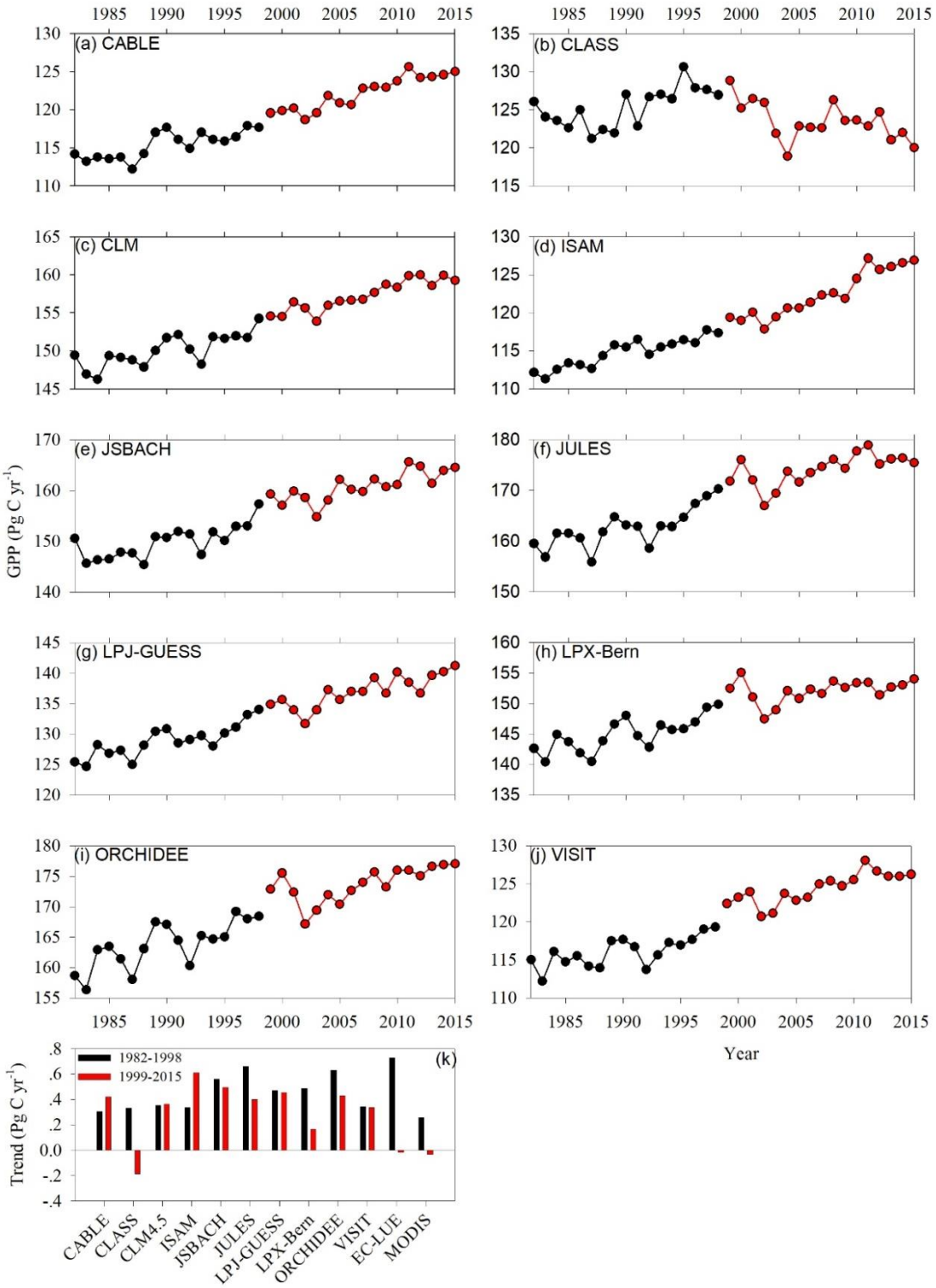

Fig. S11. Comparison on changes of global mean GPP trend simulated by ecosystem models. (**a-j**) Time series of GPP; (**k**) Changes of GPP trend for ecosystem models and two satellite-based models over the two periods of 1982-1998 and 1999-2015.

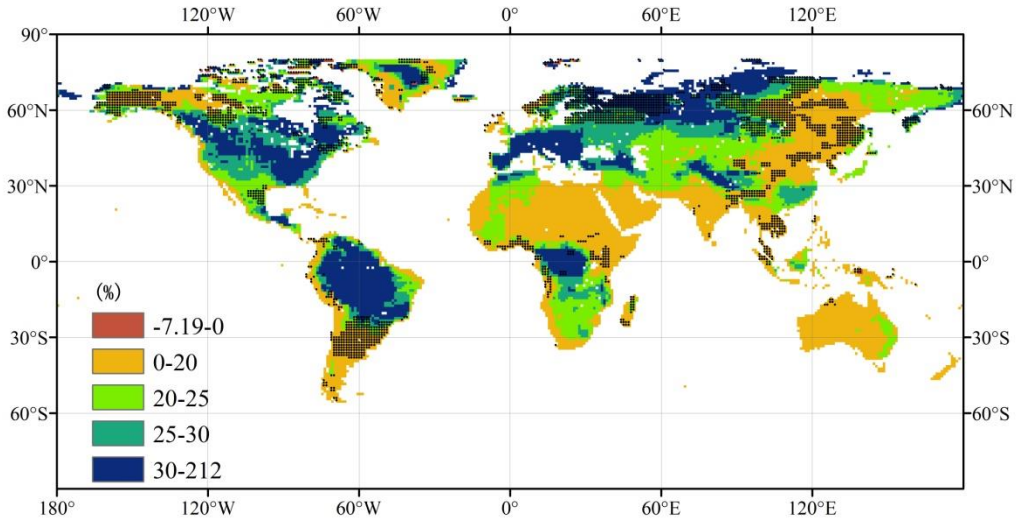

Fig. S12. Projected future changes in VPD. Percentage differences between 2080-2099 and 1980-1999 in the multimodel mean VPD simulated by six CMIP5 models under the RCP4.5 emissions scenario. Stippling indicates the areas where at least one model does not agree on the sign of the change.

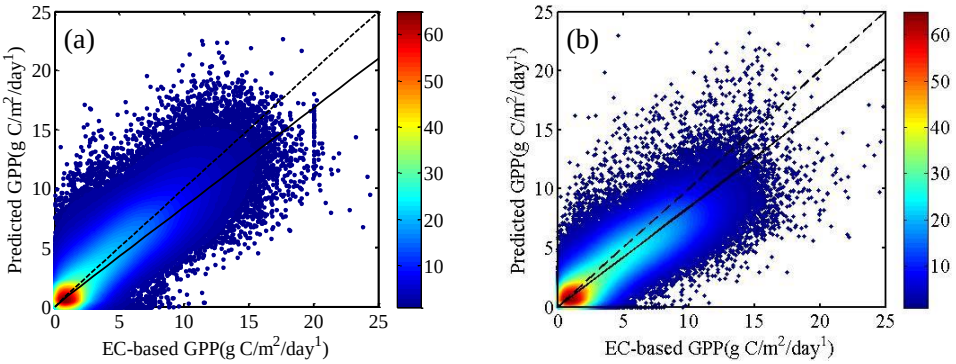

Fig. S13. Validation of EC-LUE model. Estimated GPP based on eddy covariance measurements vs. predicated GPP by EC-LUE at (**a**) model calibration sites and (**b**) validation sites in Table S4. Dashed lines are the 1:1 line and solid lines are the linear regression line. The regression relations in (a) and (b) are $y = 0.84x + 0.31$, $R^2=0.72$, $p<0.05$; $y = 0.73x + 0.55$, $R^2=0.68$, $p<0.05$, respectively.

Table S1. Climate and satellite datasets used in this study.

Variables	Dataset name	Coverage, resolution	Time span	Reference and source
Ta, AVP	CRUts3.25	Global, $0.5^{o}\times0.5^{o}$; monthly	1901 – 2015	Harris et al., 2014 *(31)* http://www.cru.uea.ac.uk/data
Ta, Td	ERA-Interim	Global, $0.125^{o}\times0.125^{o}$; monthly	1982 – 2015	Dee et al., 2011 *(33)* http://apps.ecmwf.int/datasets/
Ta, RH	HadISDH	Global, $5^{o}\times5^{o}$; monthly	1982 – 2015	Willet et al., 2012 *(32)* https://www.metoffice.gov.uk/hadobs/hadisdh/
Ta, RH	MERRA	Global, $0.5^{o}\times0.6^{o}$; monthly	1982 – 2015	Reichle, 2012 *(34)* https://disc.gsfc.nasa.gov/datasets
E_{ocean}	OAFlux	Global, $1^{o}\times1^{o}$; monthly	1958 – 2015	Yu et al., 2007 *(20)* http://oaflux.whoi.edu/
NDVI	GIMMS-3g	Global, 8km×8km; biweekly	1982 – 2015	Pinzon & Tucker, 2014 *(36)* https://ecocast.arc.nasa.gov/data/pub/gimms
LAI	GLASS	Global, $0.05^{o}\times0.05^{o}$; 8-day	1982 – 2015	Xiao et al., 2016 *(37)* ftp://ftp.glcf.umd.edu/
	GLOAMap	Global, $1/13.75°\times1/13.75^{o}$; Biweekly, 1982–1999; 8-day, 2000-2011	1982 – 2011	Liu et al., 2012 *(38)* http://www.globalmapping.org/
	LAI3g	Global, 1/12°×1/12°; Biweekly	1982 – 2011	Zhu et al., 2013 *(39)* http://sites.bu.edu/cliveg/datacodes/
	TCDR	Global, $0.05^{o}\times0.05^{o}$; Daily	1982 – 2015	Claverie et al., 2016 *(40)* ftp://eclipse.ncdc.noaa.gov/
fPAR	GIMMS-3g	Global, 1/12°×1/12°; Biweekly	1982 – 2011	Zhu et al., 2013 *(39)* http://sites.bu.edu/cliveg/datacodes/

Ta, Td, AVP, RH, E_{ocean} are land surface air temperature, dewpoint temperature, vapor pressure, relative humidity, and oceanic evaporation, respectively. NDVI and LAI are Normalized Difference Vegetation Index and Leaf Area Index. fPAR is fraction of photosynthetically active radiation absorbed by the vegetation canopy.

Table S2. Responses of GPP simulated by EC-LUE, MODIS, and TRENDY models to climate variables, satellite-based NDVI and fPAR, and atmospheric CO_2 concentration.

	GPP sensitivity[1]			Changes and impacts on GPP of 1982-1998				Changes and impacts on GPP of 1999-2015			
	EC-LUE	MODIS	TREDNY	Rate[2]	EC-LUE	MODIS	TREDNY	Rate	EC-LUE	MODIS	TREDNY
VPD	-13.82±3.12 Pg C/0.1kPa	-18.29±3.65 Pg C/0.1kPa	-4.57±7.04 Pg C/0.1kPa	0.0001±0.001 kPa/yr	-0.013±0.10 Pg C/yr	-0.018±0.15 Pg C/yr	-0.004±0.15 Pg C/yr	0.0017±0.0001 kPa/yr	-0.234±0.09 Pg C/yr	-0.310±0.11 Pg C/yr	-0.077±0.09 Pg C/yr
Ta	5.91±1.18 Pg C/℃	0.81±3.01 Pg C/℃	6.02±6.04 Pg C/℃	0.019±0.11 ℃/yr	0.112±0.12 Pg C/yr	0.015±0.09 Pg C/yr	0.114±0.18 Pg C/yr	0.024±0.06 ℃/yr	0.141±0.13 Pg C/yr	0.019±0.15 Pg C/yr	0.144±0.12 Pg C/yr
PAR	4.81±1.60 Pg C/100MJ	3.62±1.18 Pg C/100MJ	3.65±2.85 Pg C/100MJ	1.04±0.47 MJ/yr	0.050±0.04 Pg C/yr	0.037±0.05 Pg C/yr	0.037±0.09 Pg C/yr	-3.02±0.48 MJ/yr	-0.145±0.08 Pg C/yr	-0.109±0.09 Pg C/yr	-0.110±0.09 Pg C/yr
NDVI	22.82±5.03 Pg C/0.1NDVI	-	-	0.0014±0.0001	0.319±0.09 Pg C/yr	-	-	-0.0004±0.0003	-0.091±0.08 Pg C/yr	-	-
fPAR	-	15.03±3.11 Pg C/0.1fPAR	-	0.001±0.0003	-	0.150±0.08 Pg C/yr	-	0.0007±0.0002	-	0.075±0.11 Pg C/yr	-
$[CO_2]$	19.01±4.01 Pg C/100ppm	-	21.92±4.55 Pg C/100ppm	1.49±0.03 ppm/yr	0.283±0.15 Pg C/yr	-	0.326±0.16 Pg C/yr	2.02±0.01 ppm/yr	0.383±0.08 Pg C/yr	-	0.442±0.12 Pg C/yr

[1]Estimated GPP sensitivities to climate variables (VPD, Ta, and PAR), satellite-based vegetation index (NDVI and fPAR), and atmospheric CO_2 concentration ($[CO_2]$) by Eq. (20-22). [2]Change rates of six variables during the investigated periods. VPD and Ta are derived from CRU dataset, and PAR is derived from MERRA dataset.

Table S3. Name, location, and durations of the study EC sites used for revised EC-LUE model calibration and validation.

Site	Latitude	Longitude	Type	Study Period
Model calibration				
BE-Lon	50.55°N	4.74°E	CRO	2004-2011
DE-Kli	50.89°N	13.52°E	CRO	2004-2011
FI-Gri	48.84°N	1.95°E	CRO	2004-2011
US-Ne1	41.16°N	96.47°W	CRO	2001-2011
DE-Hai	51.08°N	10.45°E	DBF	2000-2011
IT-PT1	45.20°N	9.06°E	DBF	2002-2004
IT-Ro2	42.39°N	11.92°E	DBF	2002-2011
JP-MBF	44.39°N	142.32°E	DBF	2004-2005
US-Ha1	42.54°N	72.17°W	DBF	1991-2011
US-Oho	41.55°N	83.84°W	DBF	2004-2011
US-WCr	45.81°N	90.08°W	DBF	1999-2006
BR-Sa3	3.02°S	54.97°W	EBF	2000-2003
FR-Pue	43.74°N	3.60°E	EBF	2000-2011
MY-PSO	2.97°N	102.31°E	EBF	2003-2009
CA-NS2	55.91°N	98.52°W	ENF	2001-2005
CA-NS3	55.91°N	98.38°W	ENF	2001-2005
CA-SF1	54.49°N	105.82°W	ENF	2003-2006
CA-SF2	54.25°N	105.88°W	ENF	2001-2005
CA-TP1	42.66°N	80.56°W	ENF	2003-2011
CA-TP2	42.77°N	80.46°W	ENF	2003-2007
CZ-BK1	49.50°N	18.54°E	ENF	2004-2011
DE-Lkb	49.10°N	13.30°E	ENF	2009-2011
DE-Tha	50.96°N	13.57°E	ENF	1997-2011
US-Blo	38.90°N	120.63°W	ENF	1997-2007
US-Me2	44.45°N	121.56°W	ENF	2002-2011
US-Me6	44.32°N	121.61°W	ENF	2010-2011
US-NR1	40.03°N	105.55°W	ENF	1999-2011
CH-Cha	47.21°N	8.41°E	GRA	2006-2008; 2010-2011
CH-Oe1	47.29°N	7.73°E	GRA	2002-2008
CN-Cng	44.59°N	123.51°E	GRA	2007-2010
CN-HaM	37.37°N	101.18°E	GRA	2002-2004
CZ-BK2	49.49°N	18.54°E	GRA	2006-2011
DE-Gri	50.95°N	13.51°E	GRA	2004-2011
RU-Ha1	54.73°N	90.00°E	GRA	2002-2004
US-Goo	34.25°N	89.87°W	GRA	2002-2006
US-Var	38.41°N	120.95°W	GRA	2002-2011
AR-SLu	33.46°S	66.46°W	MF	2010
CN-Cha	42.40°N	128.10°E	MF	2003-2005
US-PFa	45.95°N	90.27°W	MF	1996-2011
US-Syv	46.24°N	89.35°W	MF	2001-2006
CA-NS7	56.64°N	99.95°W	SHR	2003-2005
US-KS2	28.61°N	80.67°W	SHR	2003-2006

CA-SF3	54.09°N	106.01°W	SHR	2002-2006
US-Sta	41.40°N	106.80°W	SHR	2008-2009
AU-DaS	14.16°S	131.39°E	SAV	2008-2011
AU-Ade	13.08°S	131.12°E	SAV	2008-2009
CN-Ha2	37.61°N	101.33°E	WET	2003-2005
DE-Spw	51.89°N	14.03°E	WET	2010-2011
US-Ivo	68.49°N	155.75°W	WET	2004-2007
US-Los	46.08°N	89.98°W	WET	2000-2010
Model validation				
US-Ne2	41.16°N	96.47°W	CRO	2001-2011
US-Ne3	41.17°N	96.43°W	CRO	2001-2011
US-Twt	38.10°N	121.65°W	CRO	2009-2011
US-ARM	36.60°N	97.48°W	CRO	2003-2011
FR-Fon	48.48°N	2.78°E	DBF	2005-2011
IT-Ro1	42.41°N	11.93°E	DBF	2000-2008
US-MMS	39.32°N	86.41°W	DBF	1999-2011
US-UMB	45.56°N	84.71°W	DBF	2000-2011
ZM-Mon	15.44°S	23.25°E	DBF	2007-2009
AU-Tum	35.66°S	148.15°E	EBF	2001-2011
BR-Sa1	2.86°S	54.96°W	EBF	2008-2011
CN-Din	23.17°N	112.54°E	EBF	2003-2005
AU-ASM	22.28°S	133.25°E	ENF	2010-2011
CA-NS1	55.88°N	98.48°W	ENF	2002-2005
CA-NS4	55.91°N	98.38°W	ENF	2003-2005
CA-NS5	55.86°N	98.49°W	ENF	2001-2005
CA-Qfo	49.69°N	74.34°W	ENF	2003-2010
CA-TP3	42.71°N	80.35°W	ENF	2003-2011
CN-Qia	26.74°N	115.06°E	ENF	2003-2005
DE-Obe	50.78°N	13.72°E	ENF	2008-2011
FI-Hyy	61.85°N	24.30°E	ENF	1996-2011
IT-La2	45.95°N	11.29°E	ENF	2001
IT-Lav	45.96°N	11.28°E	ENF	2003-2011
IT-Ren	46.59°N	11.43°E	ENF	1999-2004, 2009-2011
NL-Loo	52.17°N	5.74°E	ENF	1996-2011
RU-Fyo	56.46°N	32.92°E	ENF	1998-2011
AT-Neu	47.12°N	11.32°E	GRA	2002-2003; 2009-2011
AU-DaP	14.06°S	131.32°E	GRA	2008, 2010-2011
CH-Fru	47.12°N	8.54°E	GRA	2006-2008; 2010-2011
CN-Du2	42.05°N	116.28°E	GRA	2007-2008
IT-Tor	45.84°N	7.58°E	GRA	2009-2011
NL-Hor	52.24°N	5.07°E	GRA	2004-2011
US-AR1	36.43°N	99.42°W	GRA	2009-2011
US-AR2	36.64°N	99.60°W	GRA	2009-2011
BE-Bra	51.31°N	4.52°E	MF	1999-2011
BE-Vie	50.31°N	6.00°E	MF	1999-2011

CA-Gro	48.22°N	82.16°W	MF	2003-2011
CA-NS6	55.92°N	98.96°W	SHR	2002-2005
ES-LgS	37.10°N	2.97°W	SHR	2007-2009
AU-Dry	15.26°S	132.37°E	SAV	2008-2011
US-Ton	38.43°N	120.97°W	SAV	2001-2011

CRO: cropland; DBF: deciduous broadleaf forest; EBF: evergreen broadleaf forest; ENF: evergreen needleleaf forest; GRA: grassland; MF: mixed forest; WET: wetland; SAV: savanna; SHR: shrubland.

Table S4. Correlations between VPD and LUE at different temperature ranges.

Site	15-16℃[1]	16-17℃	17-18℃	18-19℃	19-20℃	20-21℃	21-22℃	22-23℃	23-24℃	24-25℃
AR-SLu	0.27, 1.15[2]	0.51, 1.40	-	6.10, 5.16	-2.85, 14.51	-0.54, 6.95*	-1.67, 6.84	-1.08, 5.14	-0.65, 4.23*	-
AT-Neu	-1.00, 4.26*	-1.11, 4.46*	-1.19, 4.80*	-0.78, 4.03*	-1.25, 5.03*	-0.49, 3.33*	-0.78, 0.37*	-0.18, 2.35	-1.45, 5.61	-
AU-Ade	-	-	-	-	-0.67, 2.34*	-	-	-	-	-
AU-ASM	-	-	-	-	-10.76, 32.52	-	-6.53, 10.62	-0.81, 2.47	-0.28, 1.92	-
AU-Dap	-	-	-	-	-	-	-	-	-0.77, 2.99*	-0.57, 2.78
AU-DaS	-	-	-	-	-	-0.57, 2.12*	-	-	-	-
AU-Tum	-0.58, 2.39*	-0.41, 2.13*	-0.12, 1.57	-0.43, 2.23*	-0.13, 1.54	-0.27, 1.93	-0.42, 2.25	-0.78, 3.29*	-0.95, 3.82	-
BE-Bra	-0.25, 1.91*	-0.36, 2.02*	-0.21, 1.82*	-0.33, 2.07*	-0.23, 1.73*	-0.46, 2.25*	-0.45, 2.18*	-0.60, 2.58*	-0.45, 2.21*	-
BE-Lon	0.03, 1.22	-0.35, 1.75*	-0.28, 1.85	-0.65, 2.37*	-0.18, 1.84	-0.55, 2.22	-0.44, 2.22	-0.11, 1.32	-1.36, 4.31*	-
BE-Vie	-0.40, 2.03*	-0.53, 2.27*	-0.47, 2.21*	-0.49, 2.21*	-0.45, 2.12*	-0.50, 2.27*	-0.72, 2.88*	-0.34, 1.89	-0.49, 2.31	-
BR-Sa1	-	-	-	-	-	-	-	-0.12, 1.84	-0.03, 1.65	0.00, 1.73
BR-Sa3	-	-	-	-	-	-	-0.74, 2.61	-0.73, 3.06*	0.56, 1.01	-0.23, 2.14
CA-Gro	-0.52, 2.16*	-0.66, 2.35*	-1.13, 3.51*	-0.57, 2.27*	-0.62, 2.36*	-0.51, 2.17*	-0.57, 2.23*	-0.72, 2.61*	-0.22, 1.39	-
CA-NS1	-0.38, 1.84*	-0.34, 1.66*	-0.54, 2.14*	-0.59, 2.25*	-0.40, 1.87*	-0.42, 1.82*	-0.30, 1.60*	-0.33, 1.64*	-0.32, 1.62	-
CA-NS2	-0.44, 1.92*	-0.35, 1.65*	-0.23, 1.37*	-0.24, 1.36*	-0.37, 1.62*	-0.48, 1.96*	-0.32, 1.56	-0.35, 1.58*	0.33, -0.31	-
CA-NS3	-0.22, 1.25*	-0.04, 0.88	-0.23, 1.23	-0.06, 0.88	0.34, -0.16	-0.15, 1.11	-0.59, 2.33*	-0.77, 2.84*	3.32, -8.17	-
CA-NS4	-0.36, 1.30*	-0.22, 1.08	-0.42, 1.38*	-0.66, 2.06*	-0.12, 0.84	-0.17, 0.98	0.37, -0.23	-0.68, 2.36*	-0.97, 3.17	-
CA-NS5	-0.61, 2.25*	-0.64, 2.38*	-0.36, 1.84*	-0.45, 1.97*	-0.40, 1.94*	-0.68, 2.67*	-0.39, 1.85	-0.17, 1.31	-1.96, 6.43	-
CA-NS6	-0.37, 1.30*	-0.42, 1.43*	-0.64, 1.89*	-0.36, 1.34*	-0.19, 1.04	-0.15, 1.01	-0.25, 1.27	-0.17, 1.00	-0.64, 2.28*	-
CA-NS7	-0.89, 2.78*	-0.38, 1.63*	-0.65, 2.31*	-0.97, 3.11*	-0.80, 2.62*	-1.05, 3.40*	-0.66, 2.55*	-0.58, 2.29	-0.35, 1.72	-

CA-Qfo	-0.30, 1.38*	-0.41, 1.55*	-0.38, 1.46*	-0.27, 1.25*	-0.28, 1.30*	-0.31, 1.30*	-0.29, 1.26*	-0.26, 1.17	-0.21, 1.10	-
CA-SF1	-0.35, 1.59*	-0.31, 1.56*	-0.31, 1.67*	-0.20, 1.48	-0.09, 1.15	-0.59, 2.34*	1.60, -2.93*	-9.67, 26.97	-	-
CA-SF2	-1.02, 3.26*	-0.44, 2.11*	-0.41, 2.08*	-0.47, 2.28*	-0.58, 2.55*	-0.22, 1.75	0.50, -0.18	-0.49, 2.35	-0.93, 3.64*	-
CA-SF3	-0.49, 1.53*	-0.19, 0.94*	-0.44, 1.54*	-0.51, 1.70*	-0.18, 0.97*	-0.28, 1.21*	-0.25, 1.17	-0.67, 2.39	-0.16, 0.98	-
CA-TP1	-0.01, 0.56	-0.20, 0.94*	-0.07, 0.63	-0.26, 1.05*	-0.16, 0.80*	-0.11, 0.79*	-0.19, 0.96*	-0.18, 0.92*	-0.08, 0.72	-
CA-TP2	-1.07, 3.06*	-0.41, 2.49	-0.52, 2.75*	-0.69, 3.16*	-0.27, 2.17	-0.48, 2.55*	-1.36, 4.11*	-0.97, 3.77*	-0.12, 1.65	-
CA-TP3	-0.23, 1.51	-0.60, 2.11*	-0.35, 1.64*	-0.44, 1.77*	-0.61, 2.14*	-0.55, 2.05*	-0.50, 2.03*	-0.41, 1.77*	-0.46, 1.94*	-0.36, 1.71*
CH-Cha	-0.78, 2.64*	-0.64, 2.53*	-1.07, 3.24*	-0.93, 3.11*	-0.23, 1.82	-0.65, 2.70*	-0.34, 1.92*	-0.79, 3.00*	0.24, 0.52	-
CH-Fru	-0.12, 1.40*	0.02, 1.22	-0.03, 1.18	-0.12, 1.43	-0.07, 1.30	-0.07, 1.11	0.35, 0.32	-0.03, 1.13	0.11, 0.59	-
CH-Oe1	-0.33, 1.75*	-0.40, 1.82*	-0.33, 1.78*	-0.64, 2.36*	-0.30, 1.65*	-0.45, 1.88*	-0.51, 2.00*	-0.64, 2.32*	-0.91, 3.14	-
CN-Cha	-0.80, 2.89*	-0.31, 2.32*	-0.49, 2.65*	-0.62, 2.86*	-0.50, 2.63*	-0.51, 2.68*	-0.36, 2.25*	-0.87, 3.36*	-0.53, 2.63	-
CN-Cng	-1.22, 4.00*	-1.01, 3.44	-0.18, 1.71	-1.37, 3.95*	-1.70, 4.95*	-0.97, 3.50*	-1.30, 4.32*	-1.51, 4.88*	-1.27, 4.34*	-
CN-Din	-	-	-	-	-	-	-	-0.40, 2.29*	-0.78, 2.35	-
CN-Du2	-0.77, 2.15*	-0.36, 1.32	-0.36, 1.30	-0.70, 2.11*	-0.38, 1.22	-0.69, 2.25*	-0.63, 1.93*	-0.04, 0.26	-0.92, 3.07*	-
CN-Ha2	-	-	-	-	-0.62, 1.93*	-	-	-	-	-
CN-HaM	-0.66, 1.86*	-	-	-	-	-	-	-	-	-
CN-Qia	-	-	-	-	-3.49, 7.43*	0.46, 1.37	18.00, 0.19	-2.42, 5.66*	-1.00, 3.93*	-
CZ-BK1	-0.37, 2.55*	-0.66, 3.08*	-0.25, 2.45*	-1.07, 3.83*	-1.17, 4.17*	-0.55, 2.82	-0.46, 2.67	-1.41, 4.58*	-1.10, 4.13*	-
CZ-BK2	-0.37, 2.02*	-0.49, 2.35*	-0.40, 2.07*	-0.47, 2.32*	-0.45, 2.27	-0.21, 1.96	-0.61, 2.71	0.61, -0.16	0.43, 0.02	-
DE-Gri	-1.23, 3.87*	-0.96, 3.37*	-1.13, 3.96*	-1.18, 3.98*	-1.22, 4.23*	-0.60, 2.78	-1.75, 5.49*	-2.00, 6.49*	-2.96, 9.17*	-
DE-Hai	-0.59, 2.86*	-0.63, 2.84*	-0.63, 2.85*	-0.81, 3.22*	-0.93, 3.54*	-0.72, 3.03*	-0.61, 2.82*	-1.41, 5.05*	-1.74, 5.94*	-
DE-Kli	-0.28, 1.76*	-0.57, 2.21*	0.05, 1.10	-0.63, 2.39	-0.68, 2.58	-0.85, 2.76*	-1.39, 4.26*	-0.90, 3.22	-0.72, 2.76	-

DE-Lkb	0.32, -0.07*	-0.06, 0.50	0.12, 0.14	0.08, 0.23	-4.88, 11.91	0.12, 0.08	0.03, 0.29	-	-	-
DE-Obe	-0.57, 2.53*	-0.37, 2.23*	-0.64, 2.70*	-0.42, 2.32*	-0.49, 2.46	-0.18, 1.95	-0.46, 2.36	-0.16, 1.70	9.44, -23.81	-
DE-Spw	-0.59, 3.30*	-0.83, 3.55*	-0.95, 3.83*	-1.36, 4.53*	-1.35, 4.55*	-0.82, 3.53*	-0.81, 3.43*	-0.55, 2.88	-0.62, 2.99	-
DE-Tha	-0.73, 3.21*	-0.93, 3.56*	-0.83, 3.27*	-0.70, 3.12*	-1.10, 3.99*	-0.89, 3.57*	-0.83, 3.38*	-0.65, 2.97*	-0.82, 3.38*	-0.71, 3.54*
ES-LgS	-0.40, 1.33*	-0.02, 0.45	-0.15, 0.73*	-0.46, 1.58*	0.08, 0.14	0.17, -0.15	-	-	-	-
FI-Gri	-	-	-	-	-0.36, 2.01*	-0.25, 1.23*	-	-	-	-
FI-Hyy	-0.45, 2.00*	-0.47, 2.03*	-0.41, 1.96*	-0.30, 1.71*	-0.52, 2.21*	-0.38, 1.92*	-0.51, 2.20*	-0.64, 2.50*	-0.18, 1.45	-
FR-Fon	-1.33, 4.51*	-0.97, 4.13*	-1.14, 4.65*	-1.12, 4.41*	-1.16, 4.61*	-0.78, 3.91*	-1.09, 4.38*	-1.38, 5.10*	-0.98, 4.17*	-
FR-Pue	-0.22, 1.37	-0.20, 1.21*	-0.16, 1.07*	-0.34, 1.42*	-0.34, 1.49*	-0.38, 1.52*	-0.35, 1.42*	-0.27, 1.16*	-0.24, 1.09*	-0.31, 1.29*
IT-La2	-0.88, 2.65*	-0.82, 2.70*	0.44, 0.09	-0.06, 0.90	0.50, -0.23	-	-	-	-	-
IT-Lav	-0.30, 1.57*	-0.39, 1.69*	-0.30, 1.52*	-0.34, 1.59*	-0.30, 1.45*	-0.54, 2.01*	-0.45, 1.79	-0.56, 2.11*	-	-
IT-PT1	-	-0.74, 2.66*	-1.28, 3.21	-0.80, 3.26	-0.28, 2.50	-0.29, 2.50	-0.47, 2.64*	-0.33, 2.48*	-0.60, 3.07*	-
IT-Ren	-0.01, 1.53	-0.24, 1.65	-0.17, 1.45	-0.62, 2.33*	-0.52, 2.11	-	-	-	-	-
IT-Ro1	-1.22, 4.25	-1.07, 3.93	-0.35, 2.34	-0.39, 2.76	-0.63, 2.87*	-0.17, 1.90	-0.48, 2.27*	-0.76, 3.09*	-0.54, 2.54*	-0.48, 2.34*
IT-Ro2	-0.84, 3.24	-0.20, 2.51	-0.16, 2.27	-0.32, 2.51	-0.81, 3.44*	0.03, 1.51	-0.17, 1.92	-0.46, 2.58*	-0.61, 2.91*	-0.30, 2.21*
IT-Tor	0.10, 0.91	-0.83, 3.12	-	-	-	-	-	-	-	-
JP-MBF	-0.60, 2.03*	-1.64, 3.60*	-0.46, 1.72*	-0.52, 1.84	-0.80, 2.56*	-0.56, 2.13*	-0.27, 1.57	-	-	-
MY-PSO	-	-	-	-	-	-	-	-	-0.15, 1.29	-
NL-Hor	-0.43, 1.85*	-0.57, 2.33*	-0.52, 2.15*	-0.30, 1.87*	-0.30, 1.83*	-0.05, 1.35	-0.01, 1.26	-0.14, 1.49	-0.50, 2.13	-
NL-Loo	-0.28, 1.85*	-0.32, 1.92*	-0.48, 2.15*	-0.37, 1.95*	-0.42, 2.06*	-0.52, 2.28*	-0.47, 2.12*	-0.46, 2.16*	-0.56, 2.42*	-
RU-Fyo	-0.48, 2.26*	-0.47, 2.22*	-0.55, 2.29*	-0.46, 2.13*	-0.60, 2.33*	-0.50, 2.12*	-0.45, 2.03*	-0.46, 2.05*	-0.51, 2.21	-0.65, 2.44
RU-Ha1	-0.31, 1.20*	-0.26, 1.09*	-0.28, 1.20*	-0.72, 2.07*	-0.09, 0.75	-0.04, 0.65	-0.05, 0.61	0.17, 0.03	0.44, -0.64	-

US-AR1	-	-	-	-1.02, 3.72	-0.18, 1.09	-0.57, 2.09	0.13, 0.22	-0.48, 1.59	-0.10, 0.93	-
US-AR2	-	-	-	-0.10, 0.94	-0.14, 0.85	-0.08, 0.62	-4.85, 10.93	-0.46, 1.43	-0.70, 2.41*	-
US-ARM	-	-	0.02, 0.57	0.13, -0.14	-1.51, 3.41*	-0.16, 1.07	-0.18, 0.88	-0.12, 0.93	-0.06, 0.79	-
US-Blo	-0.12, 0.92	-0.20, 1.02*	-0.27, 1.27*	-0.01, 0.58	-0.20, 1.13*	-0.14, 0.93	-0.26, 1.29*	-0.25, 1.21	-0.58, 2.27*	-0.83, 2.99*
US-Goo	-	-0.40, 1.43*	1.55, -1.85	-1.69, 4.04	-0.10, 1.27	-0.05, 0.93	-0.30, 1.38	-0.49, 1.82*	-0.23, 1.37*	-
US-Ha1	-0.46, 1.86*	-0.37, 1.87*	-0.37, 1.84*	-0.32, 1.82*	-0.35, 1.92*	-0.26, 1.81*	-0.29, 1.87*	-0.29, 1.87*	-0.18, 1.56*	-
US-Ivo	0.15, 0.87	-0.60, 1.75	0.02, 0.38	-4.37, 10.98	-	-	-	-	-	-
US-KS2	-	-	-	-	-	-	-	-	-0.33, 1.38	-
US-Los	0.05, 0.90	-0.11, 1.16*	-0.05, 1.04	-0.10, 1.09*	0.09, 0.75	-0.03, 1.02	0.03, 0.88	-0.26, 1.55*	-0.24, 1.47*	-
US-Me2	-0.39, 1.61*	-0.34, 1.47*	-0.28, 1.36*	-0.48, 1.94*	-0.30, 1.45*	-0.60, 2.30*	-0.92, 3.34*	-0.46, 2.01*	-1.06, 3.86*	
US-Me6	0.16, 0.12*	-0.37, 1.31*	-0.67, 2.13*	-0.30, 1.22	-0.43, 1.55*	-0.22, 1.03	-0.02, 0.45	-1.40, 4.69*	-	-
US-MMS	-0.58, 2.62*	-0.51, 2.73	-1.11, 3.79*	-0.37, 2.41*	-0.33, 2.18*	-0.92, 3.30*	-0.39, 2.35*	-0.54, 2.61*	-0.47, 2.49*	-0.50, 2.58*
US-Ne1	-0.59, 2.47*	-1.12, 3.18*	0.08, 1.40	-1.15, 3.78*	-0.82, 3.47*	-0.88, 3.54*	-0.81, 3.60*	-0.75, 3.81*	-0.75, 3.93*	-0.82, 3.94*
US-Ne2	-0.43, 1.92	-0.42, 1.85	-1.38, 3.60*	-0.92, 3.20*	-0.89, 3.02*	-0.57, 2.46*	-0.37, 2.41*	-0.83, 3.47*	-0.68, 3.19*	-0.97, 3.66*
US-Ne3	-1.19, 2.82*	-0.96, 2.30*	-0.78, 2.47*	-0.83, 2.69*	-0.48, 2.13	-0.58, 2.47*	-0.76, 2.93*	-0.73, 3.11*	-0.56, 2.78*	-
US-NR1	-0.63, 2.27*	-0.61, 2.25*	-1.02, 3.35*	-0.52, 2.05	-	-	-	-	-	-
US-Oho	-0.70, 3.12*	-0.70, 3.02*	-0.49, 2.71*	-0.54, 2.71*	-0.61, 2.95*	-0.62, 3.00*	-0.49, 2.67*	-0.54, 2.83*	-0.57, 2.96*	-
US-PFa	-0.12, 1.55*	-0.23, 1.37*	-0.30, 1.52*	-0.41, 1.73*	-0.30, 1.57*	-0.31, 1.56*	-0.38, 1.72*	-0.36, 1.66*	-0.53, 2.05*	-
US-Sta	-0.33, 1.66	0.05, 0.03	-0.01, 0.20	-0.10, 0.39	-0.01, 0.16	-0.10, 0.38	-0.11, 0.43	-0.26, 0.87*	-0.34, 1.12	-
US-Syv	-0.44, 1.73*	-0.42, 1.76*	-0.31, 1.56*	-0.38, 1.88*	-0.25, 1.64*	-0.41, 1.91*	0.03, 1.05	-0.17, 1.54	0.01, 1.23	-
US-Ton	0.49, -0.12	-0.24, 1.10	-0.31, 1.26	0.09, 0.28	-0.14, 0.77	0.15, 0.02	-0.10, 0.62	-0.17, 0.83	-0.11, 0.66	-0.09, 0.61
US-Twt	-0.55, 1.71	-4.15, 8.70*	-1.92, 5.32	-3.83, 9.59*	-2.26, 7.03*	-1.99, 6.82*	-0.66, 3.68	-1.40, 5.38	-4.23, 13.59*	-2.87, 9.76

US-UMB	-0.63, 2.55*	-0.69, 2.67*	-0.75, 2.85*	-0.64, 2.66*	-0.58, 2.53*	-0.40, 2.23*	-0.49, 2.44*	-0.71, 2.99*	-0.49, 2.48*	-
US-Var	0.17, 0.85	-0.59, 1.39	-0.38, 0.97*	-0.38, 1.02	-0.62, 1.70*	-0.60, 1.69*	-0.21, 0.69	-0.65, 2.01*	-1.05, 3.25*	-
US-WCr	-0.40, 1.44*	-0.40, 1.72*	-0.26, 1.48*	-0.39, 1.70*	-0.23, 1.42	-0.49, 1.89*	-0.34, 1.62*	-0.37, 1.68	-0.51, 2.03*	-
ZM-Mon	-	-	-	-	-0.55, 1.98*	-0.55, 2.01	-0.69, 2.04	-0.99, 2.67*	-1.02, 2.84	-1.92, 5.34

[1]air temperature ranges from 15℃-25℃. [2]correlation coefficients (a, b) of logarithm equations (LUE=a×ln(VPD)+b), and * indicates the significance level at $p<0.05$. "-" indicates failure regression due to no adequate measurements.

Table S5. CMIP5 models used to estimate VPD from 1850 to 2100.

Modeling Center/Group	Institute ID	IPCC Model Name
Canadian Centre for Climate Modelling and Analysis	CCCMA	CanESM2
National Center for Atmospheric Research	NCAR	CESM1
NASA Goddard Institute for Space Studies	NASA GISS	GISS-E2-R
Met Office Hadley Centre	MOHC	HadGEM2
Institute for Numerical Mathematics	INM	INM-CM4
Atmosphere and Ocean Research Institute (The University of Tokyo), National Institute for Environmental Studies, and Japan Agency for Marine-Earth Science and Technology	MIROC	MIROC5

Table S6. Correlation matrixes for global VPD simulated by the six CMIP5 ESMs and four historical datasets (CRU, ERA-Interim, HadISDH, and MERRA).

	CRU	ERA-Interim	HadISDH	MERRA	CanESM2	CESM1	GISS E2-R	HadGEM2	INM-CM4	MIROC5
CRU	-	0.93	0.80	0.70	0.49	0.52	0.44	0.32	0.25	0.25
ERA-Interim		-	0.89	0.76	0.38	0.47	0.47	0.40	0.07n	0.63
HadISDH			-	0.77	0.38	0.46	0.37	0.34	0.09n	0.59
MERRA				-	0.30	0.46	0.38	0.28	0.07n	0.48
CanESM2					-	0.89	0.87	0.84	0.74	0.79
CESM1						-	0.88	0.84	0.75	0.78
GISS E2-R							-	0.81	0.74	0.77
HadGEM2								-	0.69	0.74
INM-CM4									-	0.65
MIROC5										-

The correlation matrixes display correlation coefficient (R^2) of global averaged vapor pressure deficit, and "n" indicate the insignificant correlation.

Table S7. Model parameters of EC-LUE for different vegetation types.

Vegetation Type	DBF	ENF	EBF	MF	GRA	CRO	WET	SAV	SHR
ε_{max} (g C MJ^{-1})	2.02	3.16	3.92	3.46	3.32	2.85	2.65	1.54	0.75
θ (ppm)	60	20.69	30	52	75	64	68	41	37
VPD_0 (kPa)	0.54	0.69	0.29	0.41	1.21	0.89	1.16	1.04	1.13

DBF: deciduous broadleaf forest; ENF: evergreen needleleaf forest; EBF: evergreen broadleaf forest; MF: mixed forest; GRA: grassland; CRO: cropland; WET: wetland; SAV: savanna; SHR: shrubland.